Inorg. Chem. **2007**, *46*, 7899–7909

Investigations on a Novel Silyl Transfer Reaction in Heterodimetallic Chemistry†

Abdelatif Messaoudi,‡ Peter Deglmann,‡,|| Pierre Braunstein,*,‡ and Peter Hofmann*,§

Laboratoire de Chimie de Coordination, Institut de Chimie (UMR 7177 CNRS), Université Louis Pasteur, F-67070 Strasbourg Cédex, France, and Institut für Organische Chemie, Universität Heidelberg, Im Neuenheimer Feld 270, D-69120 Heidelberg, Germany

Received April 22, 2007

Heterodinuclear silyl complexes of the type $[(OC)_3(R_3Si)\overline{Fe(\mu\text{-}PPh_2)Pt}(CO)(PPh_3)]$, which contain a $\overline{Fe(\mu\text{-}P)Pt}$ triangular core, were previously reported to undergo an unprecedented dyotropic-type rearrangement involving migration of the silyl group from iron to platinum with concomitant 1,2 migration of CO from Pt to Fe. In the resulting complexes of formula $[(OC)_4\overline{Fe(\mu\text{-}PPh_2)Pt}(SiR_3)(PPh_3)]$, the Si atom occupies a cis position at the planar Pt center with respect to the phosphido bridge. DFT calculations were employed to elucidate the mechanism of this intramolecular silyl migration reaction. When the Fe–Pt precursor complex is $[(OC)_3(R_3Si)\overline{Fe(\mu\text{-}PPh_2)Pt}(PPh_3)_2]$, the reaction sequence involves (i) the substitution of PPh_3 by CO at Pt, (ii) the concerted migration of CO and SiR_3, and (iii) the cis–trans isomerization at Pt. The calculations support the exergonic character of the overall process. An explanation for the experimental observation of only one product isomer being formed is possible via frontier molecular orbital analysis. Consistent with the experimental findings, the transition states of the migration (a species with a triply bridged intermetallic bond) and isomerization steps were found to be energetically within reach at room temperature. Additional support for the suggested mechanism also comes from the fact that relative silyl migration activities could be rationalized by the means of quantum chemistry.

Introduction

Ligand migration reactions represent key steps in stoichiometric and catalytic molecular chemistry, and their mechanisms have been studied in great detail for a number of years.[1] In contrast to the dynamic behavior of ligands in fluxional molecules, where the starting and end points are chemically identical, the irreversible migratory insertion of a ligand in the coordination sphere of a metal (e.g., the migratory insertion of CO into a metal−alkyl bond or the silyl migration reactions leading to the formation of Si−C, Si−P, or Si−O bonds)[2] or the irreversible migration of a ligand from one metal center to another in a dinuclear or cluster complex generates one or more new chemical functionalities. In the latter case, the presence of chemically different adjacent metal centers opens the possibility of metalloselective transformations. Dinuclear and cluster chemistry provide unique opportunities for the study of such phenomena,[3] and both their occurrence and their rationalization at a molecular level help to delineate and better understand the mechanism of 1,2-ligand migrations taking place between adjacent sites on metal surfaces.[4−6]

Despite the importance of metal−silicon chemistry in diverse areas such as organometallic chemistry, catalysis, and materials science, *heterodimetallic* silicon chemistry has only

* To whom correspondence should be adressed. E-mail: braunstein@chimie.u-strasbg.fr (P.B.), ph@oci.uni-heidelberg.de (P.H.).

† Dedicated to Professor Roald Hoffmann on the occasion of his 70th birthday.

‡ Université Louis Pasteur.

|| Present address: Polymer Physics Department, BASF-Aktiengesellschaft, D-67056 Ludwigshafen, Germany.

§ Universität Heidelberg.

(1) Crabtree, R. H. *The Organometallic Chemistry of the Transition Metals*; John Wiley & Sons: New York, 2005.
(2) Braunstein, P.; Knorr, M. *J. Organomet. Chem.* **1995**, *500*, 21.
(3) *Metal Clusters in Chemistry*; Braunstein, P., Oro, L. A., Raithby, P. R., Eds.; Wiley-VCH: Weinheim, Germany, 1999; Vols. 1−3.
(4) Braunstein, P.; Boag, N. M. *Angew. Chem., Int. Ed.* **2001**, *40*, 2427.
(5) (a) Braunstein, P.; Rosé, J. In *Metal Clusters in Chemistry*; Braunstein, P., Oro, L. A., Raithby, P. R., Eds.; Wiley-VCH: Weinheim, Germany, 1999; Vol. 2, p 616. (b) Braunstein, P.; Rosé, J. In *Catalysis by Di- and Polynuclear Metal Cluster Complexes*; Adams, R. D., Cotton, F. A., Eds.; Wiley-VCH: New York, 1998; pp 443.
(6) (a) Bradshaw, A. M. *Surf. Sci*. **1995**, *331*−333, 978. (b) Gates, B. C. *Angew. Chem., Int. Ed. Engl*. **1993**, *32*, 228. (c) Mingos, D. M. P. *J. Cluster Sci*. **1992**, *3*, 397.

10.1021/ic700761e CCC: $37.00
Published on Web 08/22/2007

recently become a well-identified research topic.[7] Novel and unexpected features have been discovered as a result of the close proximity between silyl ligands and chemically different metal centers,[7−12] which may lead to very active catalysts.[13] In particular, an unprecedented metal-to-metal silyl migration reaction has been described in a series of phosphido-bridged Fe−Pt complexes (eq 1).[8,12] Detailed

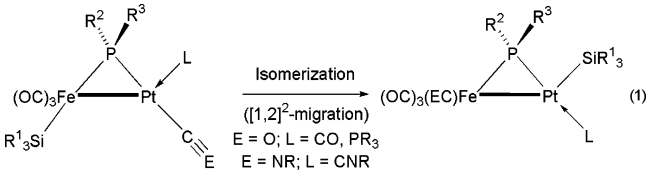

studies established that in the course of this intramolecular reaction, the silyl ligand migrates from Fe, where it is trans to the phosphido bridge, to Pt in a position cis to μ-PR^2R^3, with a concomitant 1,2 migration of CO (or in some cases CNR) from Pt to Fe. This dyotropic-type rearrangement was found to depend on the steric properties of the silyl ligand, the nature of the substituents on the phosphido bridge, and on the ligand L bound to Pt. We have elsewhere addressed the issue of an involvement of bridging silyl intermediates or transition states in these reactions, emphasizing the striking similarities and differences between the bonding modes of the isolobal fragments $(CR_3)^-$, $(SiR_3)^-$, and PR_3.[4] It was subsequently found that this silyl migration reaction was not restricted to phosphido-bridged complexes and that diphosphine ligands of the type $Ph_2PCH_2PPh_2$ are also suitable to bring the two metals close enough to enable the reaction. Also, in these cases, the Fe/Pt couple was involved.[9]

It became clear that a deeper understanding of these remarkable intramolecular ligand exchange reactions, which generate isomeric structures with complete regio- and stereoselectivity, was required. We present here a theoretical analysis of this 1,2-silyl group migration from Fe to Pt with concomitant CO migration from Pt to Fe in phosphido-bridged heterometallic Fe−Pt complexes of the type $[(OC)_3(R^1{}_3Si)Fe(\mu\text{-}PR^2R^3)PtL^1L^2]$.

Let us first summarize the relevant key experimental aspects of these reactions. When a solution of $[(OC)_3(R^1{}_3Si)Fe(\mu\text{-}PR^2R^3)Pt(COD)]$ (**1a**, R^1 = OMe, R^2 = R^3 = Ph; **1b**, R^1 = OMe, R^2 = R^3 = Cy; **1c**, R^1 = Ph, R^2 = R^3 = Ph; **1d**, R^1 = Ph, R^2 = R^3 = Cy; **1e**, R^1 = Ph, R^2 = H, R^3 = Ph; COD = 1,5-cyclooctadiene) in CH_2Cl_2 was exposed to a CO atmosphere, the corresponding complexes $[(OC)_4Fe(\mu\text{-}PR^2R^3)Pt(SiR^1{}_3)(CO)]$ (**2a**−**e**) rapidly formed, in which the silyl ligand has migrated from Fe to Pt and in which two CO ligands have been coordinated, one at each metal (eq 2).[12] When 2 equiv of *t*-BuNC was slowly added to

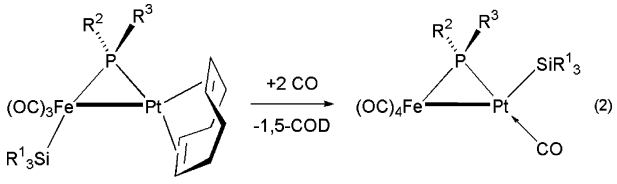

1a R^1 = OMe, R^2 = R^3 = Ph
1b R^1 = OMe, R^2 = R^3 = Cy
1c R^1 = Ph, R^2 = R^3 = Ph
1d R^1 = Ph, R^2 = R^3 = Cy
1e R^1 = Ph, R^2 = H, R^3 = Ph

2a R^1 = OMe, R^2 = R^3 = Ph
2b R^1 = OMe, R^2 = R^3 = Cy
2c R^1 = Ph, R^2 = R^3 = Ph
2d R^1 = Ph, R^2 = R^3 = Cy
2e R^1 = Ph, R^2 = H, R^3 = Ph

solutions of **1a** or **1c** at low temperature, quantitative displacement of the COD ligand was also accompanied by silyl migration from Fe to Pt and coordination of one isonitrile ligand to each Fe and Pt, leading to $[(OC)_3(t\text{-BuNC})Fe(\mu\text{-}PPh_2)Pt(SiR^1{}_3)(CNt\text{-Bu})]$ (R^1 = OMe, **3a**; R^1 = Ph, **3c**) (eq 3).[12] In all cases, the silyl ligand migrated from Fe,

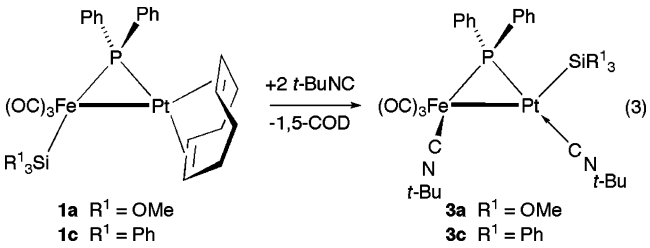

1a R^1 = OMe
1c R^1 = Ph

3a R^1 = OMe
3c R^1 = Ph

where it is trans to μ-PR^2R^3, to Pt in a position cis to the phosphido bridge. The intramolecular nature of the silyl migration reaction was established by crossover experiments.[12] The course of the silyl migration reaction was found to depend on: (a) the steric properties of the $-SiR^1{}_3$ ligand, and for a given μ-PR^2R^3 bridge (R^2 = R^3 = Ph), the migration rate decreases in the sequence $Si(OMe)_3$ > $SiMe_2Ph$ > $SiMePh_2$ ≫ $SiPh_3$; (b) the phosphido bridge, and for a given silyl ligand (R^1 = OMe), the migration rate decreases in the order μ-PPh_2 ≫ μ-PHCy; and (c) the external nucleophile, since the reaction of **1c** with 2 equiv of $P(OMe)_3$, $P(OPh)_3$, or $Ph_2PCH_2C(O)Ph$ led solely to the displacement of the COD ligand with the formation of **4a**−**c** (eq 4), respectively, whereas, as already mentioned, the reaction of **1a,c** with 2 equiv of CO or *t*-BuNC gave rise to the silyl migration.[12] The reaction of the bis(phosphine)

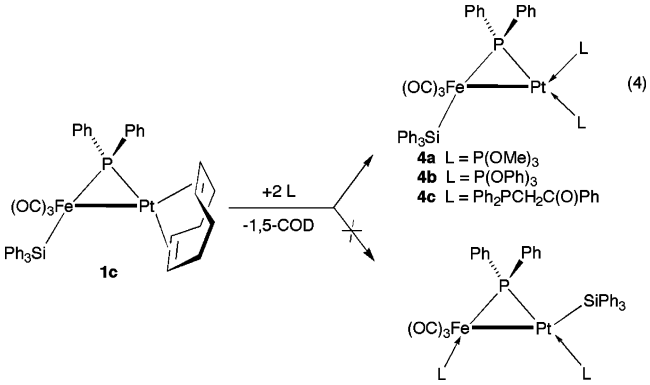

1c

4a L = $P(OMe)_3$
4b L = $P(OPh)_3$
4c L = $Ph_2PCH_2C(O)Ph$

(7) Braunstein, P.; Knorr, M.; Stern, C. *Coord. Chem. Rev.* **1998**, *178*−180, 903.
(8) Braunstein, P.; Knorr, M.; Hirle, B.; Reinhard, G.; Schubert, U. *Angew. Chem., Int. Ed. Engl.* **1992**, *104*, 1583.
(9) (a) Braunstein, P.; Faure, T.; Knorr, M. *Organometallics* **1999**, *18*, 1791. (b) Schuh, W.; Braunstein, P.; Bénard, M.; Rohmer, M.-M.; Welter, R. *J. Am. Chem. Soc.* **2005**, *127*, 10250.
(10) Knorr, M.; Braunstein, P.; Tiripicchio, A.; Ugozzoli, F. *Organometallics* **1995**, *14*, 4910.
(11) Knorr, M.; Braunstein, P.; Tiripicchio, A.; Ugozzoli, F. *Organometallics* **1996**, *15*, 2418.

complex **5a** with CO first led to **6a**, which then isomerized to the migration product **7a** (eq 5)

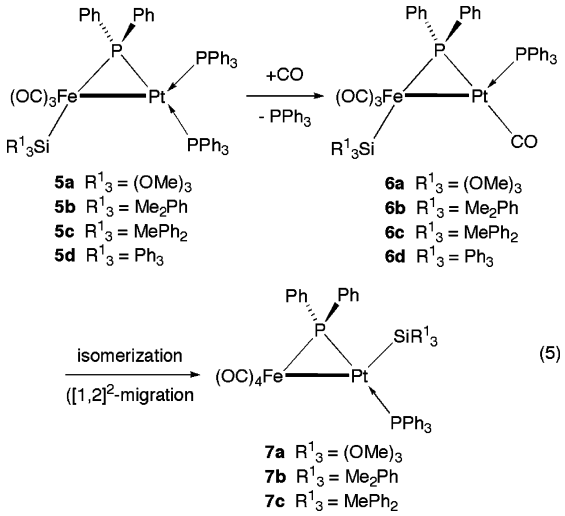

Reaction of **6e** with excess CO resulted in the opening of the Fe−Pt bond (see **8**) (eq 6).[12] In a similar manner, the

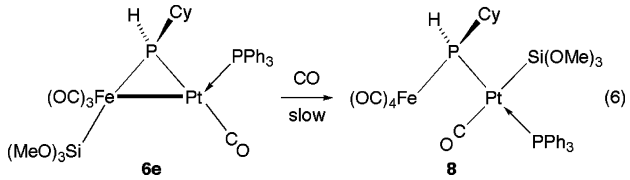

reaction of **9b** with 1 equiv of *t*-BuNC yielded [(OC)$_4$Fe(μ-PCy$_2$)Pt(CN*t*-Bu)$_2$] (**10b**) in which the metal−metal bond has been cleaved but the Pt-bound silyl ligand is trans to the phosphido bridge (eq 7)[12]

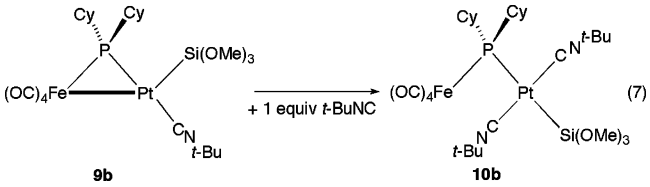

The novelty of these intramolecular silyl migrations reactions stimulated us to investigate their reaction mechanism by quantum chemical methods. The outcome of these studies is presented in the following sections.

Computational Details

All calculations were performed with the program package *Turbomole*.[14] Due to its robustness with respect to different chemical bonding situations including transition-metal complexes, we chose the DFT Becke−Perdew86 (BP86)[15−17] level of theory, which allowed us to employ the efficient RI-*J* approximation[18,19] for the Coulomb two-electron terms. For the structure optimizations we used SV(P) basis sets[20] (single-ζ for core orbitals, double-ζ for the valence shells, and one set of polarization functions for all centers except hydrogen). Single point energies were calculated with larger triple-ζ valence plus polarization basis sets (TZVP).[21] Stationary points on the potential-energy surface were characterized as either minima or transition states by the presence of zero or one imaginary frequency in the BP86/SV(P) vibrational spectrum, respectively, obtained by second analytic derivative calculations.[22,23] In addition to (nonzero point vibrationally corrected) potential energies *E* on a Born−Oppenheimer surface, we also computed Gibbs free energies *G*: all *G* values refer to 25 °C and 1 bar CO, which are the experimental conditions under which the migration reactions were observed.[12]

Scheme 1. Postulated Step in the Silyl and CO Ligand Exchange between Fe and Pt, before Ligand Isomerization at the Pt Center

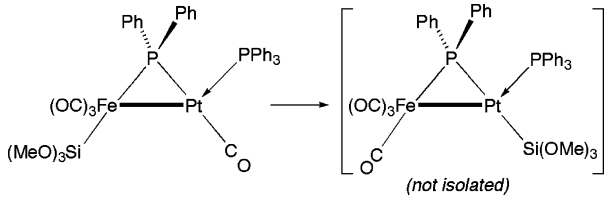

Exploring Mechanistic Pathways for a Model System

General Mechanistic Scenario. Since experimental data point to a unimolecular rate-limiting step for the silyl migration process, some kind of intramolecular exchange of a silyl group and CO between Fe and Pt should be part of the reaction mechanism (Scheme 1). Our strategy to unravel this mechanism therefore first focused on an investigation of potential structures for the complexes, intermediates as well as transition states, with bridging μ_2-silyl and/or μ_2-CO ligands. This was done with a model system where all phenyl groups at P were replaced with H atoms; at Si, however, we kept the real MeO substituents because Si−H bonds often give rise to agostic interactions with coordinatively unsaturated metal centers, which could bias the results.

All calculations point toward one (and only one) reasonable silyl transfer mechanism involving a μ_2-CO intermediate **E** from which dyotropic migration via a μ_2-silyl/μ_2-CO transition state **TS3** takes place, as shown in Scheme 2. Similar transition states involving lower coordination numbers at the metal centers, like **TS3$_{diss}$** (see Scheme 3 and the Supporting Information), were tested as well but found to play no role.

For any migration to occur, the reactant complex **A** (characterized by X-ray diffraction for the real system)[24] must

(12) Braunstein, P.; Knorr, M.; Reinhard, G.; Schubert, U.; Stährfeldt, T. *Chem.—Eur. J* **2000**, *6*, 4265.
(13) Braunstein, P.; Morise, X. *Organometallics* **1998**, *17*, 540.
(14) Ahlrichs, R.; Bär, M.; Häser, M.; Horn, H.; Kölmel, C. *Chem. Phys. Lett.* **1989**, *162*, 165.
(15) Becke, A. D. *Phys. Rev. A: At., Mol., Opt. Phys.* **1988**, *38*, 3098.
(16) Vosko, S. H.; Wilk, L.; Nusair, M. *Can. J. Phys.* **1980**, *58*, 1200.
(17) John, P. P. *Phys. Rev.* **1986**, *B33*, 8822.
(18) Eichkorn, K.; Weigend, F.; Treutler, O.; Ahlrichs, R. *Theor. Chem. Acc.* **1997**, *97*, 119.
(19) Eichkorn, K.; Treutler, O.; Oehm, H.; Haeser, M.; Ahlrichs, R. *Chem. Phys. Lett.* **1995**, *240*, 283.
(20) Schäfer, A.; Horn, H.; Ahlrichs, R. *J. Chem. Phys.* **1992**, *97*, 2571.
(21) Schäfer, A.; Huber, C.; Ahlrichs, R. *J. Chem. Phys.* **1994**, *100*, 5829.
(22) Deglmann, P.; Furche, F.; Ahlrichs, R. *Chem. Phys. Lett.* **2002**, *362*, 511.
(23) Deglmann, P.; May, K.; Furche, F.; Ahlrichs, R. *Chem. Phys. Lett.* **2004**, *384*, 103.
(24) Knorr, M.; Stährfeldt, T.; Braunstein, P.; Reinhard, G.; Hauenstein, P.; Mayer, B.; Schubert, U.; Khan, S.; Kaesz, H. D. *Chem. Ber.* **1994**, *127*, 295.

Scheme 2. Calculated Complete Reaction Cascade of the Silyl Transfer from Reactant **A** to Product **J** (Model Complexes with Ph Replaced by H at P, Minimal-Energy Pathway)[a]

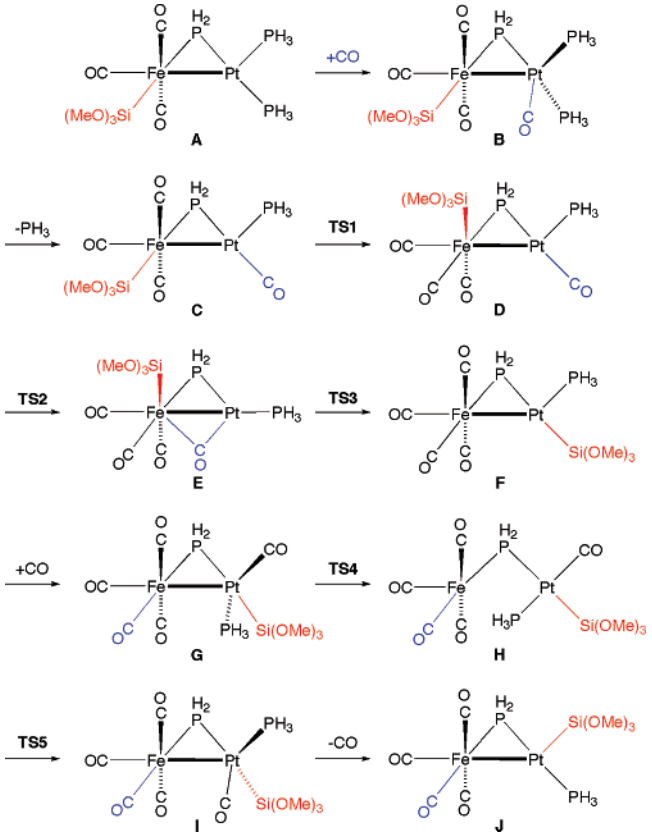

[a] See also Figure 2 for graphics of the molecular structures.

first exchange one phosphine for a CO ligand at Pt, which should occur via an associative pathway, leading to **C**. The crystal structure of a complex of type **C**, $[(OC)_3(Ph_3Si)Fe(\mu\text{-}PPh_2)Pt(CO)(PPh_3)]$, has been determined.[25] This ligand exchange is then followed by a rearrangement that makes the silyl group (at Fe) adopt an orientation orthogonal to the Fe−Pt−P triangle (as in **D**), as needed for the rate-limiting migration step. This interchange of coordination sites could proceed via a pseudorotation at Fe (main reaction path of Scheme 2) or, less likely, by CO ligand dissociation/association via a 16-electron species (vide infra). The number of complexes possibly involved in the reaction cascade is further increased by the fact that the sequence of these two transformations can be reversed. Furthermore, a cis−trans isomerization at Pt is necessary to obtain the observed product **J** from the primary migration product **F**. For this isomerization, we find two possible pathways, either via an associative mechanism (as sketched in Scheme 2) or through a unimolecular rearrangement sequence. All these alternative reaction pathways have been considered and are collected in Scheme 3. As the number of potential sideways is large, Scheme 4 gives an additional overview of possible interconversions for all species discussed in the following.

Scheme 3. Alternative Pathways for Several Sections of the Silyl Transfer Reaction Cascade (Model Complexes with H Replacing Ph at P)

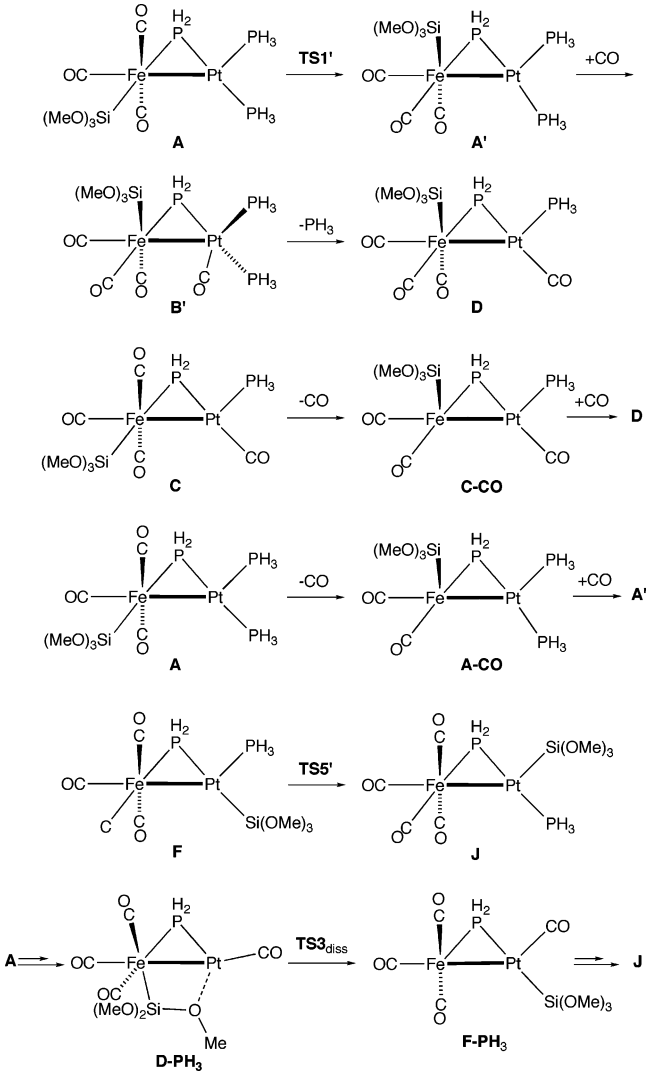

The $-Si(OMe)_3$ group exhibits C_3 symmetry, and in many cases, we have calculated the energies of the rotamers associated with this ligand. Presented here are always the most stable structures for all intermediates and transition states.

Chemical Bonding in the Dimetallic Complexes. As far as their electronic structure is concerned, all complexes involved in the silyl migration mechanism described above are clearly singlet species, with BP86/SV(P)-HOMO−LUMO gaps (HOMO = highest-occupied molecular orbital, LUMO = lowest unoccupied molecular orbital) of more than 2 eV, with the potential exception of the two rather unstable (sideways, high energy) species with a formal 16-electron count at Fe (**C**−**CO** and **A**−**CO**, both, however, still with a 1.79 eV gap) and the three structures **H** (1.85 eV), **TS5** (1.75 eV), and **TS5′** (1.15 eV)[26] in which the Fe−Pt bond is dissociating/dissociated (see Supporting Information).

There are several possibilities to describe the bonding in these complexes. In a covalent description, the neutral

(25) Reinhard, G.; Knorr, M.; Braunstein, P.; Schubert, U.; Khan, S.; Strouse, C. E.; Kaesz, H. D.; Zinn, A. *Chem. Ber.* **1993**, *126*, 17.

(26) This small HOMO−LUMO gap can be explained by additional unsaturation at the metal centers.

Scheme 4. Overview of the Potential Reaction Pathways within the Silyl Transfer Reaction Cascade

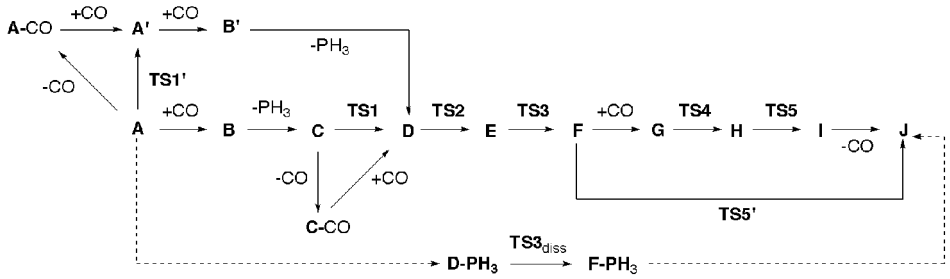

μ_2-PH_2 bridge is covalently bound to either Fe or Pt and correspondingly acts as a 2e-donor ligand to the other metal center. The ligands CO and PH_3 are two-electron donors, whereas, like the covalently bound PH_2 group, $-Si(OMe)_3$ just adds one electron to the total number and increases the formal oxidation state of the metal to which it is bound by one. Alternatively, the μ_2-PH_2 bridge could also be counted as a 4e-donor monoanion with dative bonds to both Fe and Pt.

The coordination around Fe is mainly made up of CO ligands in both **A** and **J** as well as in all intermediates and transition states between **A** and **J**, which allows the achievement, if possible, of a total valence electron count of 18 at Fe. At Pt, the often observed approximately square-planar coordination geometry corresponds to a total number of 16 valence electrons since the strongly destabilized $d_{x^2-y^2}$ orbital, which directly points toward all four ligands, is unoccupied. In reactant **A**, one counts 15 electrons at Fe and 14 electrons at Pt when omitting the PH_2 moiety. The rather short distance between these two atoms is indicative of intermetallic bonding, which (in the case of a covalent single bond) further increases the electron count by one for each metal atom. Thus, there are two electrons missing at Fe and one at Pt to achieve saturation. This would suggest that the PH_2 moiety is formally linked covalently to Pt and acts as a two-electron donor ligand toward Fe. For the final product **J** instead, again without considering the PH_2 bridge, the same consideration leads to a count of one electron missing at Fe and two at Pt, which suggests here the formation of a covalent bond between PH_2 and Fe, with two electrons being donated to Pt.

The other complexes can be viewed in an analogous way to that of **A** or **J**. A distinction between the two different situations from structural parameters, however, is not always possible because the two metal atoms are not only linked via the PH_2 unit but also directly by their intermetallic bond. Both M−P bonds and the Fe−Pt bond are strongly liable to trans influence; i.e., their lengths drastically depend on the nature of the group situated in trans position with respect to the metal center.

When assuming a covalent description of the bonding between the silyl or the phosphido ligand and the metals, in all complexes, two substituents are covalently linked to the metal atoms. Unless one assumes an identical (group−) electronegativity for Fe and Pt, in all structures one of the metals is in a formal oxidation state of +II and the other is in a state of zero. On the basis of the metal coordination geometries, it is reasonable to assign these formal oxidation states to Pt and Fe, respectively. The intermetallic bond then formally corresponds to a d^8-Fe(0) → d^8-Pt(II) dative interaction. Alternatively, each metal center could be viewed as in the (+I) formal oxidation state and the metal−metal bond as covalently linking d^7-Fe(I)−d^9-Pt(I) centers. Along the reaction cascade, this assignment will not change, irrespective of the choice of the mutual charge assignment. Therefore, the silyl migration cannot be discussed in terms of a redox reaction.

Another, equally valid qualitative description of bonding in **A** and **J** would consider all three fragments of the triangular complexes, namely, $[Fe(CO)_3Si(OMe)_3]^-$ and $[Fe(CO)_4]$ (both d^8-ML_4), as well as $[Pt(PH_3)_2]$ or $[Pt(PH_3)Si(OMe)_3]^-$ (both d^{10}-ML_2) and a PH_2^+ group as isolobal to CH_2. In this description, **A** and **J** are to be viewed as dimetallacyclopropane structures, and silyl migration is not a redox reaction either.

There are also a number of species along the reaction path, where one CO, as an additional two-electron donor, is attached to Pt. In some cases, this leaves the Fe−Pt−P triangle intact (as in **B**, **G**, **I**), which means an 18-valence-electron environment at Pt (though at least one donor ligand is rather weakly bound in this case, as will be obvious from Table 2), whereas in **H** the intermetallic bond has dissociated, which again means a square-planar 16-electron Pt complex.

The complexes with only 16 valence electrons and an open coordination site at Fe, like **C−CO** and **A−CO**, which represent potential intermediates en route to a coordination site interchange of the silyl group and one CO ligand, are rather high in energy.

Potential-Energy Profile of the Rearrangement Reaction. The "main reaction mechanism" as already summarized in Scheme 2 corresponds to the computed minimum-energy pathway. We will first consider the potential energies (i.e., without zero-point vibrational corrections), which are (together with the Gibbs free energies) listed in Table 1; the profiles are also displayed graphically in Figure 1. The addition of CO to **A** leads to **B** in a slightly exothermic reaction. Also the overall substitution of PH_3 by CO, which is accomplished in **C**, is exothermic by −19.8 kJ/mol with respect to **A**. For the subsequent coordination site interchange of the silyl and one CO ligand at Fe (eventually leading to **D**), in principle, various mechanisms are possible. The energetically most favorable way to accomplish this interconversion is a unimolecular pseudorotation (**TS1**), in this case, a rotation of the silyl group and all three CO ligands

Table 1. Calculated Potential Energies E and Gibbs Free Energies G (T = 25 °C, P_{CO} = 1 bar) for Intermediates and Transition States (BP86/TZVP||BP86/SV(P), Model Complexes with Ph at P Replaced by H)

	A	**B**	**C**	**TS1**	**D**	**TS2**	**E**	**TS3**	**F**	**G**	**TS4**
rel E (kJ/mol)	0	−20.6	−19.8	+33.5	−31.1	+26.0	+23.9	+56.6	−35.4	−86.3	−85.8
rel G (kJ/mol)	0	+22.6	+11.6	+72.4	+5.6	+64.0	+58.6	+93.0	−2.1	−1.9	+0.7

	H	**TS5**	**I**	**J**	**TS1′**	**A′**	**B′**	**C−CO**	**A−CO**	**TS5′**	**TS3$_{diss}$**
rel E (kJ/mol)	−99.8	−49.3	−97.3	−63.7	+54.2	−1.7	−34.0	+152.2	+182.2	+49.8	+131.7
rel G (kJ/mol)	−20.4	+34.9	−23.1	−31.6	+62.1	−2.0	+15.0	+124.6	+159.9	+83.4	+134.9

with respect to the Fe−Pt−P triangle. The activation barrier for this rearrangement amounts to only +53.3 kJ/mol. At much higher energy (with E more than +150 kJ/mol above **A**) are the intermediates **C−CO** and **A−CO** of the dissociative pathways. In both cases, CO removal leads to spontaneous migration of the silyl group to the free coordination site orthogonal to the triangle (and the remaining orthogonal CO ligand moves to the former silyl coordination site), which probably minimizes destabilizing trans interactions with the formally anionic silyl group. Although CO dissociation (as well as recoordination) should proceed without additional energetic thresholds, all CO ligands at Fe are so tightly bound that a dissociation should play no role compared with the pseudorotation alternative. The actual silyl and CO interchange from one metal to the other starts from **D**: first, the CO at Pt moves toward the Fe atom and thus changes from an end-on to the μ_2-CO coordination of intermediate **E**. The energy of the transition state between **D** and **E** (**TS2**) very much resembles the product, which is not surprising since the doubly bridged structure **E** is 55.0 kJ/mol less stable than **D**.

The transition state connecting **E** and **F**, in which the silyl migration has finally taken place, turns out to be the highest point of the potential-energy profile (**TS3**, E = +56.6 kJ/mol with respect to **A**). Its structure is characterized by a triply bridged (μ_2-PH$_2$, μ_2-CO, and the μ_2-silyl group) heterodimetallic arrangement. In contrast to CO, which can bind in an end-on and a μ_2 manner, a hypercoordinated Si atom is involved in **TS3** which represents a saddle point on the potential-energy surface. With the formation of **F**, the initial unrestrained Fe−Pt−P triangle is restored, which means a stabilization of 92.0 kJ/mol with respect to **TS3**. In

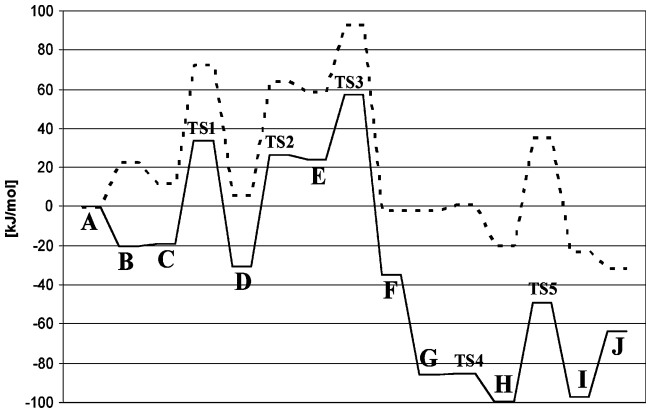

Figure 1. Calculated potential-energy E (solid line) and Gibbs free-energy G (T = 25 °C, P_{CO} = 1 bar, dashed line) profiles (BP86/TZVP||BP86/SV(P)); model complexes with Ph replaced by H at P.

experimentally observed complexes, however, the silyl group occupies a trans position with respect to the Fe−Pt bond, as in the model compound **J**. The calculations predict that **J** is preferred over **F** (by $\Delta E_{\mathbf{F}\rightarrow\mathbf{J}}$ = −28.3 kJ/mol); a rationalization of this effect will be given in a section below dealing with the molecular orbital (MO) background of complex stabilities. We therefore also performed a DFT study of possible scenarios for this cis−trans isomerization.

Just as in the CO/PH$_3$-substitution process, the cis−trans isomerization of the silyl ligand takes place at Pt, suggesting that an associative mechanism could be operative as well (with carbonyl ligands being temporarily available from the CO atmosphere necessary to cause the silyl migration). Several calculations of possible CO adducts of **F** (or **J**) yielded isomers **G** and **I**, which upon loss of CO yield **F** and **J**, respectively. The rotation of the Fe−Pt−P triangle with respect to the other three ligands at Pt from **G** to **I** was found to be a reaction sequence involving two transition states (**TS4** and **TS5**) and a ring-opened intermediate (**H**). It should be noted that **H** is more stable than both **G** and **I**, which again underlines the stability of a 16-valence-electron square-planar Pt center. **TS5** represents the maximum on the potential-energy surface in this rearrangement section of the reaction cascade with an overall barrier $\Delta E_{\mathbf{G}\rightarrow\mathbf{TS5}}$ of +37.0 kJ/mol. For the cis−trans isomerization, however, a unimolecular rearrangement transition state was also located: **TS5′**, in which the dimetallic bond is heavily stretched, directly connects **F** and **J**, but is required to overcome an activation threshold of 85.2 kJ/mol with respect to **F**, which far exceeds the barrier of the associative rearrangement.

We also examined whether a donor solvent molecule like THF could induce the cis−trans isomerization from **F** to **J** via temporary association. However, the oxophilicity of Pt is very low: a transition state (analogous to **TS5**) could be identified; it connects the intermediates of interest, but is rather high in energy (E_{rel}= +54.4 kJ/mol with respect to **A**). Owing to the additionally unfavorable entropy factor (intermediate THF coordination), the isomerization will not proceed this way, but will happen in the absence of CO (or isonitriles) via the (slower) unimolecular pathway along **TS5′**.

Gibbs Free-Energy Profile of the Reaction Cascade. Although potential energies E are the initial outcome of any potential-surface studies, all relevant properties at finite temperatures and pressures are linked to Gibbs free energies. As already mentioned, for the computed G values, we chose a temperature of 298 K and a pressure of 1 bar. As the reaction does not take place in an ideally diluted gas phase, we modified the standard statistic thermodynamic G expres-

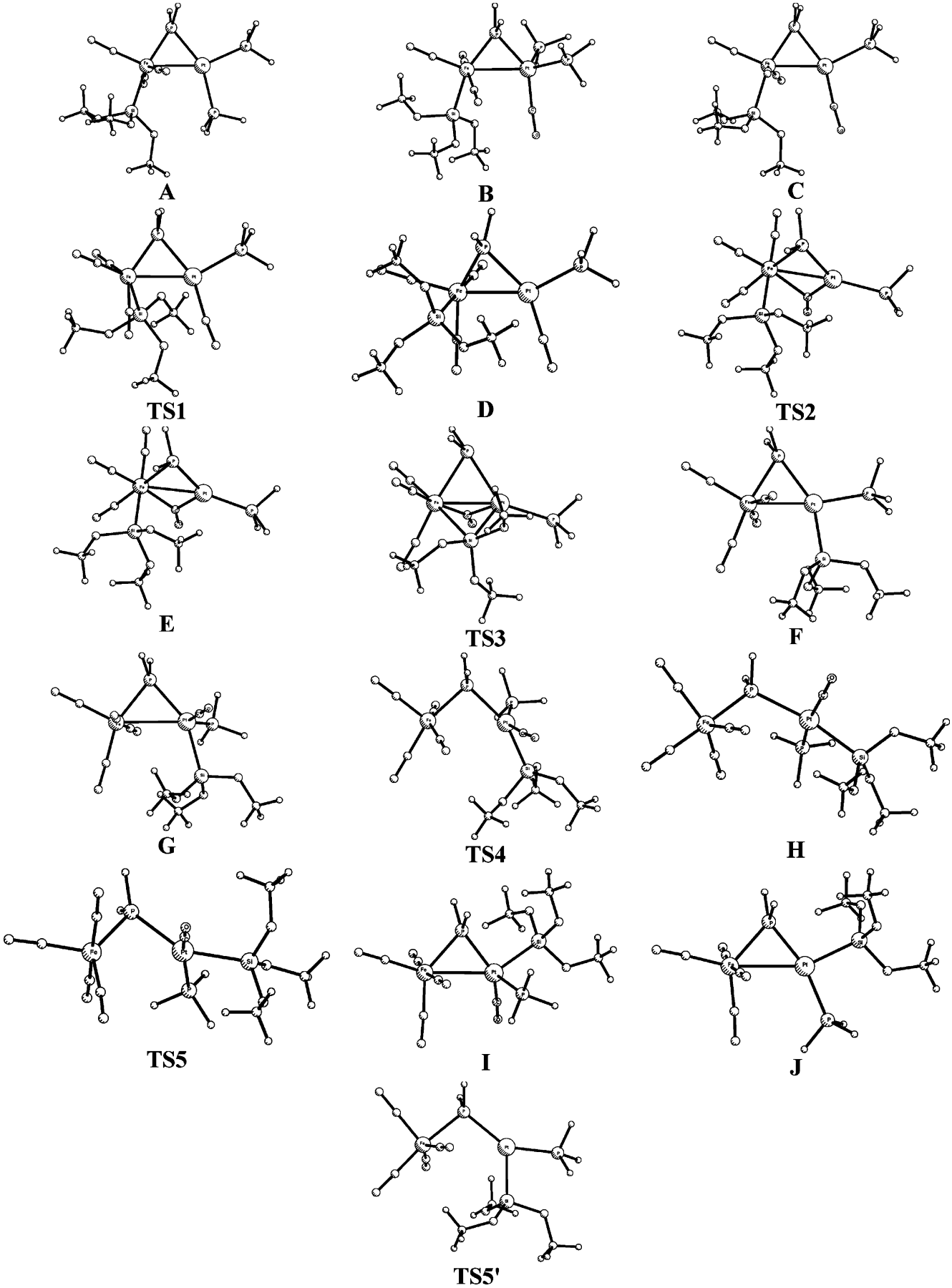

Figure 2. Structures of all model complexes along the minimum-energy pathway of Figure 1 and of the unimolecular cis−trans isomerization transition state **TS5′**.

Table 2. Selected Calculated Bond Distances (Å) for Intermediates and Transition States (BP86/SV(P), Model Complexes with Ph Replaced by H at P)

	d(Fe-μ_2-PH_2)	d(Pt-μ_2-PH_2)	d(Fe−Pt)	d(M−Si)	d(Pt−PH_3)
A	2.199	2.326	2.2682	2.304	2.345[a] 2.308[b]
B	2.187	2.368	2.806	2.328	2.381/2.476[c]
C	2.198	2.359	2.673	2.325	2.346[d]
TS1	2.161	2.318	2.729	2.366	2.327
D	2.190	2.351	2.690	2.356	2.349
TS2	2.394	2.350	2.684	2.374	2.263
E	2.484	2.351	2.724	2.389	2.255
TS3	2.479	2.484	2.622	2.729[e] 2.510[f]	2.290
F	2.335	2.432	2.631	2.345	2.276
G	2.294	2.398	3.010	2.398	2.359[g]
TS4	2.287	2.411	3.334	2.398	2.348
H	2.291	2.460	3.959	2.411	2.351
TS5	2.334	2.459	3.203	2.373	2.370
I	2.285	2.326	2.932	2.362	2.499[h]
J	2.274	2.284	2.919	2.325	2.318
TS1′	2.161	2.292	2.758	2.351	2.361 2.295 2.331
A′	2.192	2.318	2.710	2.347	2.312
B′	2.186	2.360	2.840	2.350	2.391/2.456
C−CO	2.211	2.353	2.662	2.234	2.380
A−CO	2.211	2.318	2.683	2.217	2.312 2.354
TS5′	2.310	2.388	3.583	2.347	2.238
$TS3_{diss}$	2.125	2.410	2.550	2.430	

[a] Species trans with respect to μ_2-PH_2; the upper number refers to this PH_3 ligand also for **TS1′**, **B′**, and **A−CO.** [b] Species trans with respect to Fe. [c] d(Pt−CO) = 1.938 Å. [d] d(Pt−CO) = 1.932 Å. [e] M = Fe. [f] M = Pt. [g] d(Pt−CO) = 1.913 Å. [h] d(Pt−CO) = 1.920 Å.

sion for PH_3 by omitting here the translational partition function to account for, at least in a rough approximation, the fact that the real ligand PPh_3 will not leave the reaction mixture as a gas.

As expected, the most characteristic difference between *E* and *G* is that the Gibbs free-energy profile is shifted upward with respect to the potential energy as soon as one molecule of (gaseous) CO is consumed (**B**−**F** and **J**). As a consequence, at 298 K and 1 bar, the alternative pathway from **A** to **D** with the pseudorotation (**TS1′**) before the replacement of PH_3 by CO (**A′** and **B′**) is slightly more favorable than the minimal *E* path. The maximum of the potential-energy curve, **TS3**, is also the highest point of the Gibbs free-energy profile. The moderate overall activation barrier $\Delta G_{\mathbf{A}\rightarrow\mathbf{TS3}}$ of +93.0 kJ/mol means that silyl migration can occur via the computationally proposed mechanism at room temperature.

Scheme 5. Calculated Reaction Cascade of the Silyl Transfer from the Crystallographically Characterized Reactant **5a** to the Final Product **7a**

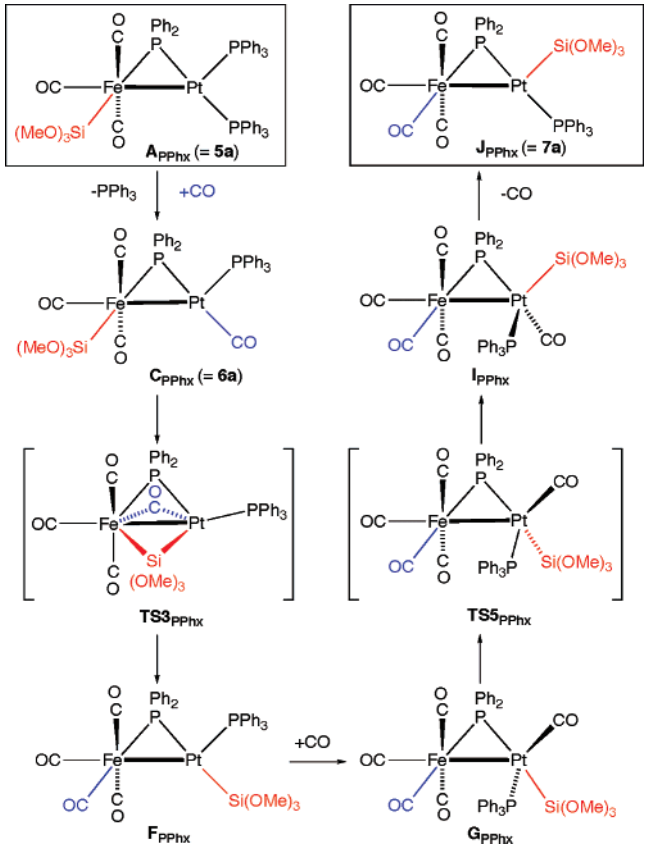

A last point concerns Gibbs free-energy changes in the cis-trans isomerization sequence, which in the case of the associative mechanism is further increased with respect to the *E* profile: here, two more CO molecules than in **A** are attached to the dimetallic complex. The minimum-energy pathway **F** → **G** → **TS4** → **H** → **TS5** → **I** → **J**, however, remains most favorable also from a *G* point of view at the chosen reaction conditions, since the opening of the Fe−Pt bond in **TS5′**, which results in coordinative unsaturation at both metal centers, induces a large destabilization.

Structural Features of Intermediates and Transition States. The structures of all intermediates and transition states along the minimum-energy pathway are shown in Figure 2. Relevant bond distances of all complexes are given in Table 2. For the Fe−P distance, we observe a clear distinction between structures **A**−**D** of the reaction cascade, where the

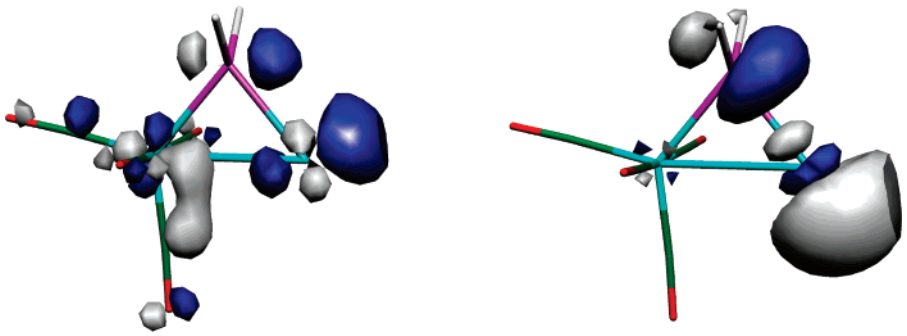

Figure 3. Contour plots of the BP86/SV(P)-α-SOMO of a [$(OC)_4$Fe(μ_2-PH_2)Pt] fragment, orbital energy = −4.68 eV (left), and of the BP86/SV(P)-α-LUMO of a [$(OC)_4$Fe(μ_2-PH_2)Pt] fragment, orbital energy = −3.53 eV (right).

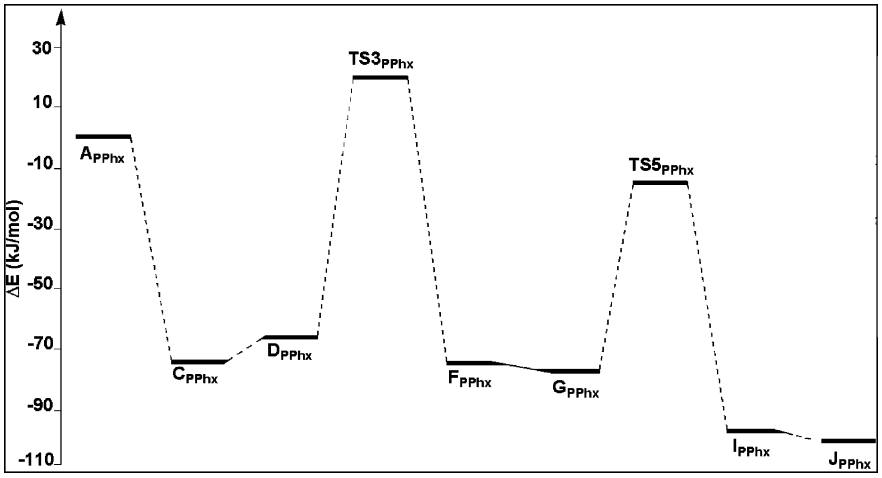

Figure 4. Calculated *E* (potential-energy) profiles for the reaction **5a** → **7a**, i.e., PPh_2 bridge and L = PPh_3 (BP86/TZVP||BP86/SV(P)) in kJ/mol.

Table 3. Calculated Potential Energies *E* for Intermediates and Transition States for the Reaction **5a** → **7a**, i.e., PPh_2 Bridge and L = PPh_3 (BP86/TZVP||BP86/SV(P))

	A_{PPhx}	C_{PPhx}	D_{PPhx}	$TS3_{PPhx}$	F_{PPhx}	G_{PPhx}	$TS5_{PPhx}$	I_{PPhx}	J_{PPhx}
ΔE (kJ/mol)	0	−74.0	−66.4	+19.7	−75.1	−77.3	−15.0	−97.7	−98.2

Table 4. Selected Calculated Bond Distances (Å) for Intermediates and Transition States (BP86/SV(P))

	d(Fe-μ_2-PPh_2)	d(Pt-μ_2-PPh_2)	d(Fe−Pt)	d(M−Si)	d(Pt−PPh_3)
A_{PPhx}	2.202	2.330	2.790	2.290	2.410[a] 2.340[b]
C_{PPhx}	2.215	2.370	2.670	2.300	2.380
D_{PPhx}	2.230	2.350	2692	2.340	2.380
$TS3_{PPhx}$	2.489	2.420	2.640	2.680[c] 2.550[d]	2.310
F_{PPhx}	2.342	2.430	2.640	2.360	2.310
G_{PPhx}	2.320	2.410	2.860	2.390	2.390
$TS5_{PPhx}$	2.359	2.520	2.760	2.410	2.380
I_{PPhx}	2.318	2.310	2.960	2.370	2.600
J_{PPhx}	2.324	2.310	2.840	2.310	2.360

[a] Species trans with respect to μ_2-PPh_2. [b] Species trans with respect to Fe. [c] M = Fe. [d] M = Pt

interaction between phosphorus and iron can be viewed as a dative P → Fe bond, and the remaining complexes, from **TS2** to **J**, where the Fe−P distance is at least 0.1 Å longer. The bond distance between Pt and μ_2-PH_2 does not show clear trends, although it also varies to some extent.

The intermetallic bond exhibits the largest variation within the structure manifold. Because it represents the weakest bond (the softest stretching potential) within the Fe−P−Pt triangle, it easily opens up (at least in some cases) if, e.g., in the cis−trans isomerization, the coordination of an additional CO group provides saturation at the metal centers without the necessity of an intermetallic interaction. Also, in the case of the unimolecular cis−trans isomerization (**TS5′**), the Fe−Pt bond dissociates, which reflects the fact that for complexes with 16 electrons formally at Pt a tetrahedral coordination is disfavored. Apart from this, the trans influence is rather pronounced for the intermetallic bond (viz., the much longer Fe−Pt distance in **J** as compared with that of **F**). The M−Si distances are rather similar for M = Fe and M = Pt. As should be expected in **TS3** with a pentacoordinate Si atom, both M−Si bonds are rather long: here, the Si atom is already closer to Pt than to Fe.

Typical M−CO distances are in the range 1.75−1.8 Å (M = Fe) and 1.9−1.95 Å (M = Pt). The μ_2-CO ligand in **TS3**, migrating in the opposite direction with respect to the moving silyl group, is closer to Fe (d_{Fe-CO} = 1.954 Å) than to Pt (d_{Pt-CO} = 2.047 Å), whereas in **E** it is attached to Pt and interacts only weakly with Fe (d_{Fe-CO} = 2.087 Å and d_{Pt-CO} = 1.992 Å). The distances between Pt and the model PH_3 ligand(s) vary between 2.25 and 2.4 Å, except for structures **B**, **B′**, and **I**, where (at least one of the) PH_3 is rather weakly bound, as the transition from 16 to 18 valence electrons at Pt strongly increases antibonding interactions (binding to the CO ligand seems unaffected by this, maybe due to the π-accepting character of CO). The shortest Pt−P distances are observed in the structures where only one terminal (phosphine) ligand is attached to Pt (**TS2** and **E**).

Molecular Orbital Background of Silyl Migration Product Stabilities. To rationalize the aforementioned preference of **J** (silyl group trans to the intermetallic bond) with respect to **F** (cis isomer), we performed an analysis of the molecular orbitals of a [$(OC)_4Fe(\mu_2$-$PH_2)Pt$] fragment, omitting both −Si$(OMe)_3$ and PH_3 ligands. For this fragment, we used the structure of **J** without these two ligands; however, it was also made sure that (i) another [$(OC)_4Fe$-(μ_2-PH_2)Pt] fragment geometry derived fom **F** (as well as a consideration of charged fragments) yielded similar results and (ii) other orbitals of similar local symmetry are energetically well-separated from the frontier orbitals.

Although the fragment has an open-shell structure with one unpaired electron, its α- and β-MOs are rather similar in shape and energy, with MO energy eigenvalues of the singly occupied MOs (SOMOs) showing a gap of only 0.62 eV. We will focus here on the α-MOs. Contour plots of the

Table 5. Calculated Potential Energies and, in Parentheses, Estimated[a] Gibbs Free Energies (both in kJ/mol) for Relevant Intermediates and Transition States Starting from Various "Real" Heterodinuclear Complexes of Composition $[(OC)_3(R_3Si)Fe(\mu\text{-}PPh_2)Pt(PPh_3)_2]$

substitution pattern	$-Si(OMe)_3$, μ-PPh_2-	$-SiPh_3$, μ-PPh_2-	$-Si(OMe)_3$, μ-P(H)(Cy)$-$
$\mathbf{A_{real}}$	0	0	0
$\mathbf{C_{real}}$	−74.0 (−39)	−92.6 (−58)	−74.8 (−40)
$\mathbf{D_{real}}$	−66.4 (−31)	−75.0 (−40)	−91.9 (−57)
$\mathbf{TS3_{real}}$	+19.7 (55)	+ 2.8 (+38)	+16.4 (+51)
max energetic spread	93.7	95.4	108.3

[a] Estimated by adding +35 kJ/mol to *E*, which is the average difference between energy and Gibbs free energy for the model compounds C, TS1, D, TS2, E, TS3, and F (which all exhibit the same atomic composition).

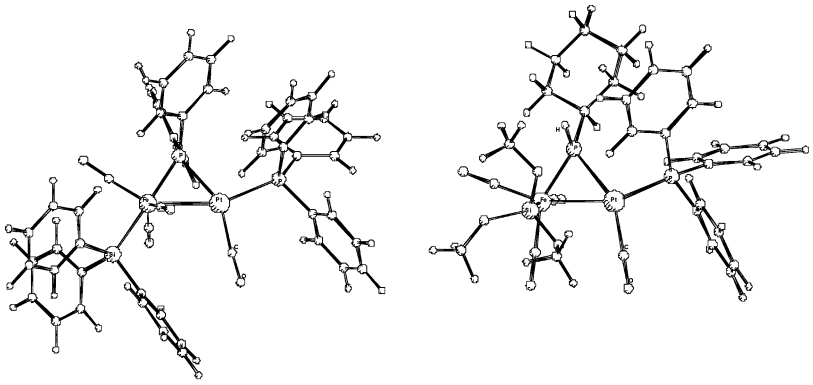

Figure 5. Structures of very stable intermediates in the case of $-SiPh_3$ and μ_2-PHCy substitution.

SOMO and LUMO are shown in Figure 3. The SOMO at Pt is strongly hybridized to the trans direction with respect to the intermetallic bond, which clearly indicates that a covalently bound ligand like the silyl group will prefer this position. On the other hand, the LUMO points toward a coordination site trans to the PH_2 bridge; a phosphine donor ligand is therefore best accommodated here. At the chosen BP86/TZVP||BP86/SV(P) level of theory, **J** is almost 30 kJ/mol more stable than **F**, where PH_3 and $Si(OMe)_3$ are arranged in the disfavored way.

Calculations Involving PPh_3 Ligands. With these findings, it is rather clear that also in the case of the experimentally studied complexes with a μ_2-PPh_2 bridge and PPh_3 ligands, triply bridged transition states such as **TS3** will represent the rate-determining step for the silyl migration. To ensure that this mechanism also allows for the isomerization of the "real" complexes, we performed calculations (illustrated in Scheme 5) of the most important steps on the pathway shown in Scheme 4, from **5a** to **7a** (structural numbering used in the introduction).

The relevant potential energies are given in Table 3, and the corresponding profiles are illustrated in Figure 4.

These results obtained for the PH_x model system therefore represent already a good approximation for the properties of the real system, as can be seen from a comparison between Table 3 and Figure 4 for the energetics and between Table 4 and the data from previous sections for the structural properties, despite the strong simplification made by replacing Ph with H.

Factors Influencing the Silyl Migration Ability. The similar shapes of the potential-energy profiles of the model system and one of the complexes studied in the experiment (see above) suggests that the migration reaction should proceed similarly for systems with other silyl substituents and phosphido bridges, e.g., those presented in the Introduction. We therefore also tried to reproduce the observed order of reactivities by further quantum chemical calculations, as another verification for our mechanism. This was done for the "less-reactive silyl substituent" $-SiPh_3$ (leaving the μ_2 phosphido bridge unchanged) and for the "less-reactive phosphido bridge" μ_2-P(H)(Cy) in combination with a $-Si(OMe)_3$ group.

Upon inspection of the *G* profile for the model system, one should expect that a higher energetic difference between species like reactant **A** and **TS3** correlates with a lower silyl migration ability, as the Gibbs free energy of **A** is lower than that for any other complex before **TS3**. As soon as the exchange of PPh_3 against CO has taken place, the *G* curve is shifted by ca. +35 kJ/mol with respect to *E*. Upon replacement of H by Ph, however, CO coordination becomes strongly exothermic and therefore *G* should also become negative for the formation of **C** and **D** from **A**. This implies that relative silyl migration abilities depend on the maximum energetic spread between either **C** or **D** and **TS3**.

The results of these investigations are shown in Table 5. A common feature to the two systems with either $-SiPh_3$ or μ_2-P(H)(Cy) is a highly stable intermediate $\mathbf{C_{real}}$ or $\mathbf{D_{real}}$, which should account for the lower reactivity of these complexes. It is noteworthy (i) that the increased stability of $\mathbf{C_{real}}$ with $-SiPh_3$ clearly is a consequence of a release of steric repulsion due to the smaller CO ligand (ii) and that in the case of μ_2-P(H)(Cy), the most stable isomer of $\mathbf{D_{real}}$ has the $-Si(OMe)_3$ group on the same side as the H atom of the

phosphido bridge. This leads to a minimization of steric repulsion, and the silyl group is "locked" in this particularly favorable "pocket". The graphics of these two thermodynamic sinks are shown in Figure 5.

Note the relative stability of $\mathbf{TS3_{real}}$ for $-SiPh_3$, in which the phenyl groups at Si and the phosphido bridge can avoid each other much better than in $\mathbf{D_{real}}$.

A comparison of the computed energies confirms a much higher energetic spread for μ_2-P(H)(Cy). The energetic difference between $\mathbf{C_{real}}$ and $\mathbf{TS3_{real}}$ is also higher for $-SiPh_3$ than for $-Si(OMe)_3$, but gas-phase energy differences of only 2 kJ/mol are easily compensated by other factors in the condensed phase; therefore, the calculated stabilities do not unambiguously explain why a $-SiPh_3$ substituent leads to lower reactivities than $-Si(OMe)_3$.

Conclusions

DFT calculations were employed to elucidate the mechanism of an unusual and unprecedented intramolecular metal-to-metal silyl migration reaction. When starting from complexes **A** (e.g., **5a**), the reaction should proceed via (i) replacement of PPh_3 by CO at Pt, (ii) concerted migration of CO and SiR_3, and (iii) cis−trans isomerization at Pt.

The calculations were able to support the exergonic character of this process. An explanation for the observation of a single isomer being formed was made possible by frontier molecular orbital analysis. Also, the transition states for both the ligand migrations (transition state with a triply bridged intermetallic bond) and the subsequent isomerization should be energetically within reach at room temperature.

Acknowledgment. This work was initiated during a visiting professorship of P.H. in the laboratory of P.B. at the Université Louis Pasteur in Strasbourg and was completed during a research stay of A.M. at the Organisch-Chemisches Institut of the University of Heidelberg. P.H. gratefully ackowledges the hospitality of the colleagues in Strasbourg. The Strasbourg Laboratory is grateful to the CNRS and the Ministère de la Recherche for financial support and to Dr. M. Knorr for initial synthetic work in the field.

Supporting Information Available: Additional tables and illustrations in PDF format. This material is available free of charge via the Internet at http://pubs.acs.org.

IC700761E